Space Calibration of Standard Solar Cells Using High-Altitude Balloon Flights

J. A. ZOUTENDYK*
Jet Propulsion Laboratory, California Institute of Technology, Pasadena, Calif.

The difficulty of predicting space power output from solar cells by means of terrestrial measurements is compounded by the complex nature of the sun's spectrum and the solar-cell spectral response. When a radiometer, such as a pyrheliometer, is used to scale the power measurements to space, large errors are possible. The radiometer is best replaced by space-calibrated standard solar cells. Such standard silicon solar cells have been obtained using high-altitude balloon flights, with accuracies of ±0.60% or better.

Introduction

SINCE the beginning of space exploration by the United States in 1958, solar cells have been the main source of electrical power for unmanned space vehicles. However, the accurate prediction of the power available from solar cells operating in space has not been possible until recently. The extrapolation of earth-based current measurements to space conditions by using total radiation detectors, such as pyrheliometers, has been particularly difficult. Since terrestrial sunlight is unlike that which exists in space in both spectral and total intensity, correction factors must be applied to the current-pyrheliometer ratios derived from measurements made in terrestrial sunlight in order to obtain space currents. Likewise, any simple source of artificial light is unlike space sunlight in both spectrum and intensity, requiring the use of correction factors.

The necessary correction factors[1] must be calculated using measurements of: 1) the spectral distribution of the light used for the cell tests, and 2) the spectral response of the cells being tested. The measurement of item 1 is difficult to perform with accuracy greater than ±5%. This measurement has proven to be impractical in sunlight at the earth's surface since changes in the spectrum occur continuously. The measurement of item 2 is also difficult to perform with accuracy greater than ±5%. Thus, in calculating the necessary correction factors, errors of ±10% are possible.

The duplication of the solar spectrum, as it exists outside the earth's atmosphere, is a possible means of testing solar cells. Problems arising from this duplication are: 1) the limited accuracy with which the sun's spectrum is known, 2) the difficulty in duplicating the sun's spectrum because of its complex structure, and 3) duplicating the sun's spectrum uniformly over large areas with the same degree of collimation that exists in space, which is not now possible.

A solution to the problem of extrapolating solar-cell current measurements to space conditions is the replacement of the pyrheliometer with a standard solar cell in which the space short-circuit current is known. A standard solar cell, calibrated for space sunlight, need only have a spectral response that is representative of those cells being tested. As the art of manufacturing solar cells has become more sophisticated, the uniformity of the product has improved. Through careful control of crystal growth, junction diffusion, and other manufacturing processes, a higher yield of uniform and efficient solar cells has been achieved. Whereas five years ago a single production lot of a few hundred solar cells would exhibit a wide range in spectral response, today as many as 100,000 solar cells may have practically identical spectral sensitivity. The convergence of spectral response in silicon solar cells over the years has enhanced the feasibility of using a few calibrated standard solar cells to predict both the individual and the integrated power output of a large number of cells.

The space calibration of standard cells has been performed with good success using high-altitude balloon flights. This paper discusses the results of three balloon flights performed by the Jet Propulsion Laboratory for solar-cell space calibration.

Balloon Flight System for Solar-Cell Measurements

High-altitude balloon flights have been used extensively as a research tool to investigate phenomena of celestial origin, such as the measurement of energetic nuclear particles (cosmic rays).[2] By using high-altitude balloons, it is possible to make observations of extraterrestrial phenomena which have been altered very little by our atmosphere. Specifically, the response of solar cells to space sunlight may be observed with good correlation to their performance in outer space.

The foremost consideration in designing a balloon flight system for solar-cell measurements is the maximum or floating altitude of the flight. At an altitude of 80,000 ft above sea level, the total solar intensity is only 0.5% less than in space for wavelengths to which a silicon solar cell is responsive (0.4 to 1.2 μ). Taking into account the structure of the solar spectrum and silicon solar-cell spectral response, the decrease in a solar-cell's space short circuit is less than 0.3% at this altitude. To obtain an altitude of 120,000 ft, the balloon diameter must be three times that for 80,000 ft and the volume 27 times greater. An altitude of 80,000 ft was chosen for the three flights discussed in this paper.

The actual size of the balloon is determined by its total weight and flight hardware. A balloon can support more weight attached on the bottom than on the top. However, there are disadvantages in mounting solar cells on the bottom of the balloon. One disadvantage is that a payload mounted on the bottom is subject to pendulum and torsional motion, making the tracking of the sun for solar-cell illumination more difficult. Another is that, when positioned at the bottom of the balloon, solar cells are exposed to sunlight reflections from the main body of the balloon. Although a lighter payload must be carried on the top of a balloon than on the bottom, the problems of reflections from the balloon and solar-tracker instability for a bottom-mounted payload are severe enough to justify mounting the solar-cell payload on the top. Only those instruments that are absolutely neces-

Presented as Preprint 2504-62 at the ARS Space Power Systems Conference, Santa Monica, Calif., September 25–28, 1962; revision received January 28, 1965. This paper presents the results of one phase of research carried out at the Jet Propulsion Laboratory, California Institute of Technology, under Contract No. NAS 7-100, sponsored by NASA.

* Senior Research Engineer.

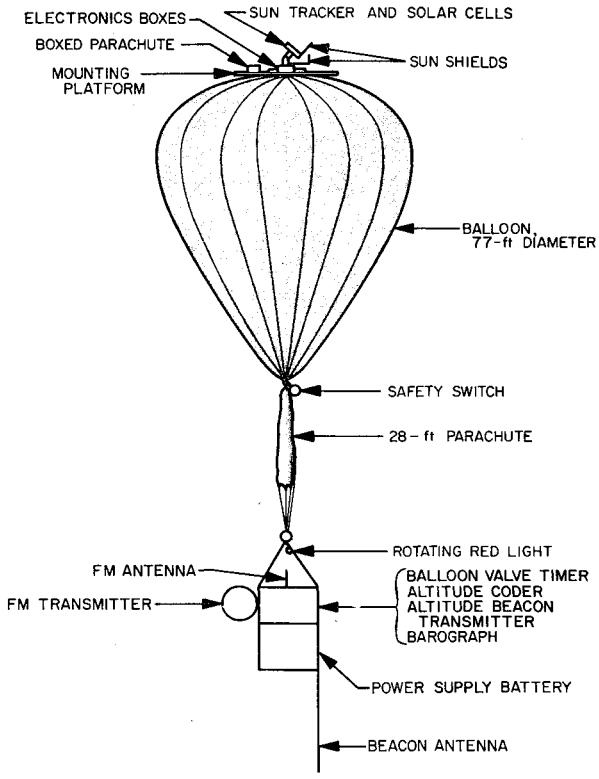

Fig. 1 Balloon flight system.

sary to the sun-tracker assembly, plus lightweight pieces of equipment, are mounted on top of the balloon. Heavy items, such as power supply batteries and transmitter, are carried on a bottom-mounted gondola.

Figure 1 illustrates the over-all system used for the three balloon flights discussed in this paper. The system is divided into three major components: 1) balloon, 2) the balloon-mounted data-acquisition system, including the solar tracker, the batteries for the power supply, and the balloon-mounted telemetry system, and 3) the ground-based telemetry system, which receives and decodes signals from the balloon transmitter.

The type of balloon used for the three flights is constructed using 1.5-mil-thick polyethylene. Each balloon, when fully inflated, is 77 ft in diameter and has a maximum capacity of 175,000 ft^3. The amount of helium used to lift the balloon is determined by total system weight. The balloon is inflated with enough gas to provide a lifting force which is 10% greater than the force of gravity on the total system. The amount of helium needed to fulfill this requirement is 7150 ft^2 at standard temperature-pressure (STP). The weight of the balloon alone is 185 lb.

The balloon-mounted, data-acquisition system is centered around the solar tracker upon which the solar cells are mounted. Prior to the actual flight, the solar tracker is tested extensively on the ground to determine the accuracy of solar alignment that it can achieve. These tests show that a maximum 2° sun-angle change needs to occur for the tracker to correct. In addition to this, the sun-orientation accuracy of the tracker is 2°. Considering both aspects of the solar-tracker operation, the maximum angle of misorientation is 4°. When the tracker is operated in sunlight on earth, the sun shadow-image on the tracking sensors is not as well defined as it is in the well-collimated sunlight at high altitudes. Therefore, it is reasonable to expect that the tracker should operate better in the virtually parallel light rays of the sun when the balloon is at maximum altitude as compared to the highly diffused light that reaches the ground. A photoresistance detector is mounted on the tracker as an indicator for an off-sun condition. The photoresistor is used to modulate a 1-kc audio-oscillator, which generates a 60-cps signal tone when the tracker is off the sun by 3°. The tone increases to 2000 cps for a misorientation of 6°.

During a flight, data are transmitted from the balloon via an FM-FM telemetry system (Fig. 2). There are 24-individual measurements, which are sequenced through a stepping switch. These measurements consist of: 1) three solar-cell temperatures, 2) 14 solar-cell, short-circuit currents (voltage across a 1.000 ± 0.001-Ω resistor), and 3) seven precision standard voltages for inflight calibration purposes.

The solar-cell temperature measurements are derived from the voltage across a thermistor. The first flight had three separate thermistors mounted on control cells for temperature measurements. For the last two flights, one of the thermistors was replaced by a 174-kΩ resistor, providing a calibration for the telemetry temperature data.

The standard voltages, plus the voltages from the test cells and thermistor circuits, are fed into a voltage-controlled oscillator (VCO) through a stepping switch. The VCO is a stable oscillator whose frequency is a linear function of the voltage at its input terminals. For a 0-v input, the frequency of the VCO is 7882 cps. The frequency drops to 6806 cps for an input signal of 100 mv, which corresponds to a 10.8-cps change in frequency for a 1-mv change in signal. The audio tone used to indicate an off-sun condition of the solar tracker is transmitted on a separate frequency band. The off-sun frequency is generated by a VCO, which is independent of the main VCO used for the preceding 24 measurements. Standard voltages are maintained by using temperature-compensated zener diodes that have been selected for precise voltages and low temperature coefficients. Prior to flight, the standard voltages are adjusted to within ±0.01% of their calibration value. The inflight calibration voltage circuit is temperature-controlled to stay within 30 to 40°C during flight. For this temperature range, the standard voltages are maintained with an accuracy of ±0.1%. The temperature of the main VCO is maintained between 35 and 45°C during flight, thereby controlling frequency drift. The standard voltages on the balloon provide a highly accurate data system, even in the event of frequency drift in the VCO. The stepping switch, through which the 24 measurements are sequentially fed, advances one step every 15 sec. Since there are 24 positions in the switch, a complete cycle is executed every 6 min. The output frequency from the VCO is fed into a 225-Mc FM transmitter, as shown in the block diagram in Fig. 2. The frequency output from the VCO is added to the 225-Mc signal of the transmitter, which sends the FM signal to the receiving station located on the ground. The signal received on the ground is fed into a preamplifier,

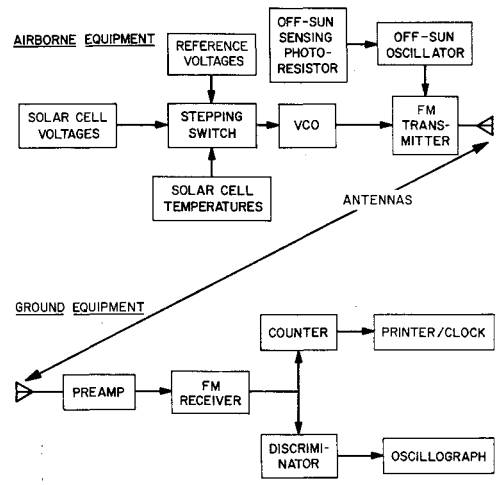

Fig. 2 Balloon telemetry system block diagram.

and then into an FM receiver. The output of the FM receiver is displayed in two parallel forms: 1) through a counter and printer/clock combination, and 2) through a discriminator and oscillograph system. The counter-printer/clock combination will read frequency to ±1 cps, which corresponds to a ±0.093-mv reading accuracy of the VCO input voltage. The discriminator-oscillograph system is less accurate, but provides a graphic readout of the data. The balloon-mounted telemetry system is tested in an environmental chamber at temperatures ranging from −35 to +65°C. Within this temperature range, the standard voltages remain constant to within ±0.1%.

The payload mounted on top of the balloon is shown in Fig. 3. Mounted with the solar tracker are two electronics boxes (one on either side of the tracker), which house the thermistor voltage network, the VCO's, the stepping switch, and the standard voltage circuit. The total weight of the top payload, including the mounting platform, is 40 lb. The mounting platform was increased in size for the last two flights. The diameter was changed from 4 to 6 ft to provide a better mounting base for the top payload. The box with the parachute was removed for the third flight.

The weight of the 28-ft parachute and safety switch (Fig. 1) is 20 lb. During descent, the bottom payload is cut away from the balloon with the safety switch and allowed to parachute to the ground. The weight of the bottom payload, which includes the gondola, the power supply batteries, the FM transmitter, and other instruments, is 170 lb. Incidental items mounted on the balloon provide a weight of 10 lb, giving a total system weight of 425 lb.

The ground receiving equipment for the telemetry system is located in a bus stationed at the launching site. The telemetry system is capable of transmitting and receiving signals over a direct line distance of 250 miles. If necessary, the ground-based telemetry bus is moved to stay within the receiving radius of the transmitter. Tracking equipment is maintained in a panel truck, which is used to follow the balloon. A small aircraft is also held in readiness to track the balloon, if necessary.

Balloon Flight Solar Cells

Special solar-cell modules were fabricated for the solar-cell measurements made on the balloon flights. One of the modules is shown in Fig. 4. Each module contains two solar cells, each of which is loaded with a 1.000 ± 0.001-Ω precision resistor. When loaded with a 1-Ω resistor, the current from each cell is essentially the short-circuit current. Therefore, the voltage across the 1-Ω resistor is proportional to the short-circuit current of the cell. Each resistor has a temperature coefficient of less than 0.0001 Ω/°C.

Several different types of cells were flown on the first balloon.[3] Among them were cells with both deep and shallow diffused junctions. Some of the cells were flown uncovered, whereas others were flown with a 0.006-in.-thick glass sheet covered with an interference filter that reflected light below a certain wavelength. Filters with both 450- and 410-mμ cutoffs were used. The cells flown on the first flight were both P/N and N/P silicon solar cells. On the second and third flights, only P/N silicon solar cells were used. Two of the cells flown on the first flight (SM 6-9 and SM 6-10) were also used on the second and third flights. These cells were reflown on all three flights to establish the reproducibility of the measurements. For each cell flown, the relative equal-energy spectral response was measured. Figure 5 shows the spectral response of the two cells flown repeatedly on the three balloon flights. One of the cells (SM 6-9) was uncovered; the other (SM 6-10) was covered with a 450-mμ filter. Both of these cells are P/N, shallow-diffused, silicon solar cells. The presence of a 450-mμ filter on SM 6-10 is apparent in its spectral response shown in Fig. 5. Spectral response measurements made on the solar cells before and after the flights indicated no significant change in the spectral characteristics during the flights. The solar-cell payload flown on the first balloon flight is shown mounted on the solar tracker in Fig. 6.

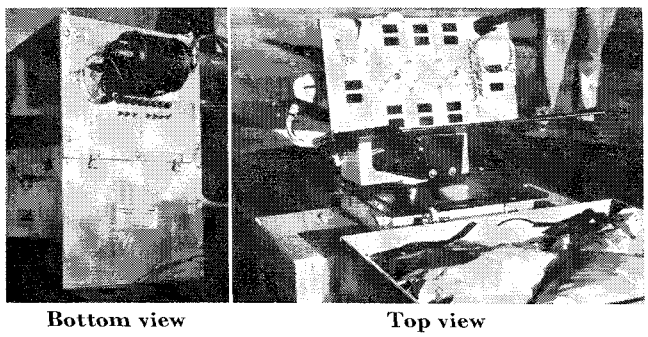

Bottom view Top view

Fig. 3 Top and bottom, mounted payloads.

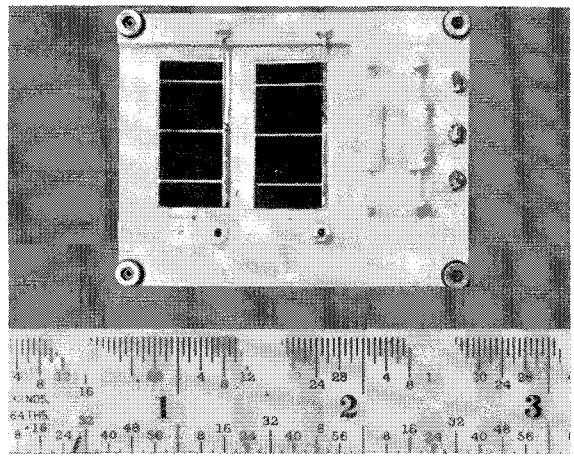

Fig. 4 Solar-cell module for balloon flights.

Balloon Flight Performance

The three balloon flights for solar-cell evaluation took place on June 13, 1962,[3] August 6, 1963, and September 5, 1963. All three of the flights were preceded by a preflight test of the telemetry system. The preflight calibration of the standard voltages has already been mentioned. A continuity check of the total system, starting from the output of the cells and going through the stepper switch to the output of the main VCO, was performed in the laboratory.

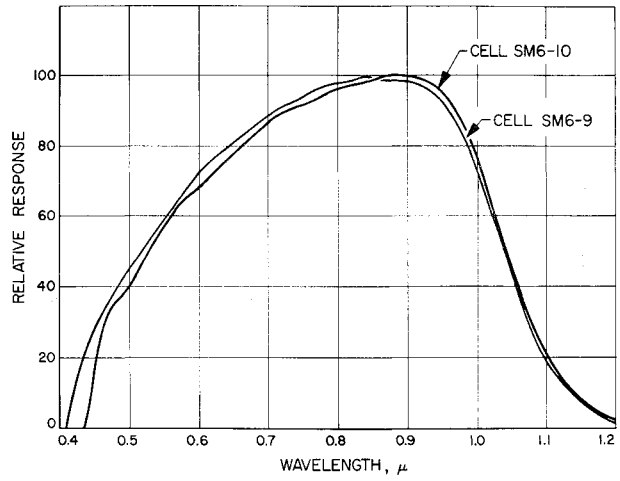

Fig. 5 Relative spectral response for SM 6-9 and SM 6-10.

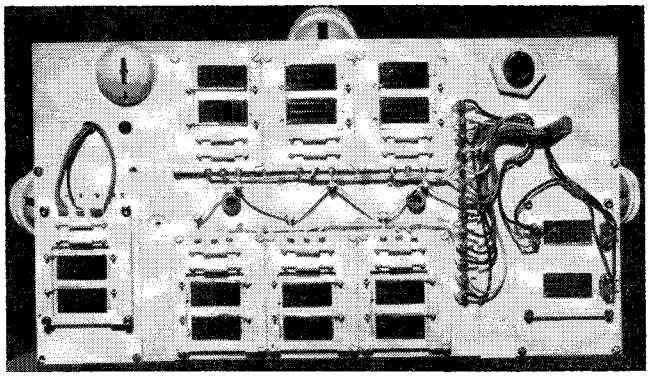

Fig. 6 Solar-cell payload for first flight.

Prior to launching, a check was made again at the launch site on the telemetry system, starting with the output of the cells and going through the output of the VCO. The preflight ground check-out also included the transmission of data through the ground-based telemetry equipment. In addition, the solar tracker was vigorously tested at the launch site. Upon verification of the proper operation of all of the components, the balloon was inflated. During inflation, the final balloon lift calculations were made to determine the exact rate of ascent. On the first balloon flight, an operator's error caused an extra tube of helium to be put into the balloon. With the extra lift from the helium, the rate of ascent might have been too great for the balloon to withstand. Therefore, a ballast weight of 50 lb was hung on the end of the balloon gondola, allowing for the proper rate of ascent of the balloon. However, the added weight caused a reduction in maximum altitude from 80,000 to 77,000 ft.

At approximately 4 hr before solar noon, the balloons were released from the tethering apparatus. During the ascent of the balloon (Fig. 7), the sun tracker oriented itself toward the sun, except during rewind periods. (The sun tracker must rewind after the balloon makes three complete rotations in either the clockwise or counterclockwise direction.)

During ascent the balloon is not yet expanded to maximum volume. Hence, there is a certain amount of balloon material which can reflect sunlight onto the solar cells and the tracker sensors. This tends to nullify the data taken during the ascent portion of the flight.

During the three flights the solar-cell temperatures reached a minimum of $-10°C$ at an altitude around 50,000 ft. This phenomenon was caused by a cold layer that exists in the atmosphere, known as the troposphere. The balloon altitude as a function of time for the third flight is shown in Fig. 8. Upon reaching maximum altitude of around 80,000 ft, the balloons remained there for 3 to 4 hr around solar noon. During this time, the solar heating of the gas in the balloons caused a partial venting of the helium. This, in turn, caused a small altitude loss, which did not alter the solar-cell short-circuit current or temperature readings. The venting of gas is necessary to keep the balloons from exploding. During the floating period, 30 to 40 data points were obtained on each of the 24 measurements. About 2 hr after solar noon, the balloons were brought down by a radio command that released helium through a port in the top. During descent, the balloons were tracked with the system in the panel truck. Within minutes after landing, the balloons were recovered and the payloads removed. After securing the solar tracker and other gear in the panel truck, the cells were examined and returned to the laboratory for further examination and dismantling from the tracker. No damage was incurred by the solar cells during the three flights.

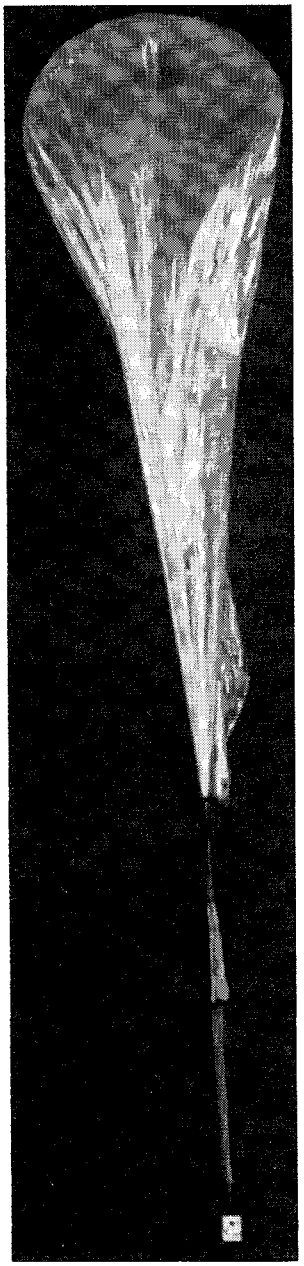

Fig. 7 Balloon launch.

The data from the first balloon flight indicated that some of the cells were possibly seeing reflections from the top of the balloon, even at maximum altitude. To prevent reflec-

Table 1 Balloon flight data for SM 6-9 and SM 6-10

Flight date	SM 6-9 average I_{sc}, ma	SM 6-9 rms deviation, %	SM 6-10 average I_{sc}, ma	SM 6-10 rms deviation, %	Solar-cell temperature, °C	R, a.u.	L, mw/cm²
6-13-62	62.08	±0.28	59.19	±0.29	19 ± 1	1.0156	135.3
8-6-63	62.86	±0.40	59.68	±0.37	32 ± 1	1.0143	135.7
9-5-63	63.04	±0.13	60.17	±0.08	32 ± 1	1.0083	137.3

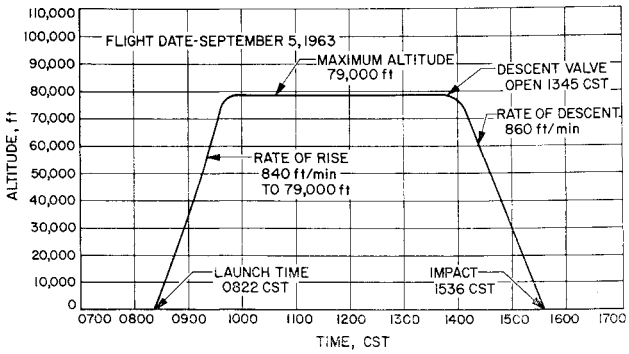

Fig. 8 Balloon altitude vs time for third flight.

tions from the balloon, the second flight carried a sun shield mounted on the face of the tracker. Also, the platform used to mount the payload on top of the balloon was increased in diameter and painted black. In addition, an extra "cap" of polyethylene material was placed on the top of the balloon, hopefully to prevent the formation of "bulges" that could reflect light onto the solar cells. However, the data from the second flight exhibited even more scatter than was observed on the first flight. The polyethylene cap was believed to be causing reflections onto the solar cells rather than preventing them. Therefore, the cap was omitted for the third flight. The data from the third was very stable, indicating that the reflections from the balloon had been eliminated.

The stabilized temperature measurements at maximum altitude on the second flight were 12° to 14°C higher than those on the first flight. This was a direct result of the high absorptivity of black paint on the mounting platform. For the third flight, the platform was painted gray, instead of black, hopefully to decrease the temperature of the cells. No decrease in temperature was observed on the third flight.

Discussion of Balloon Flight Data

During the three balloon flights discussed in this paper, short-circuit current data on 38 individual solar cells were obtained. Some 30 to 40 short-circuit current measurements at 80,000 ± 3000 ft above sea level were obtained on 36 of the 38 cells. For two of the cells, SM 6-9 and SM 6-10, approximately 100 short-circuit current data points at floating altitude resulted from the three flights. The data obtained from all 38 solar cells provided a calibration of each as a primary space standard for terrestrial solar-cell measurements.

During the first flight, the solar-cell temperatures stabilized at 19° ± 1°C for the last hour of maximum altitude.[3] The

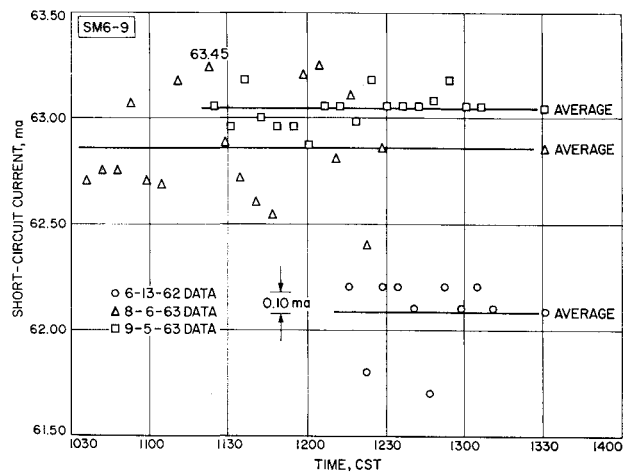

Fig. 9 Temperature-stabilized data, SM 6-9.

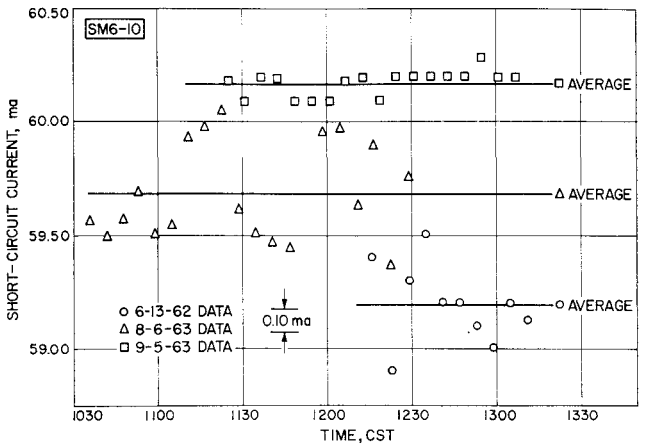

Fig. 10 Temperature-stabilized data, SM 6-10.

10 data points obtained for each cell during this time are shown in Figs. 9 and 10. During the last two flights, the cells stabilized at 32° ± 1°C for about the last 2 hr of float. These points are also shown in Figs. 9 and 10. Table 1 lists the average value of the temperature-stabilized, short-circuit currents (I_{sc}) and the root-mean-square (rms) deviation of all of the data points from the average. In the same table, the earth-sun distance R in astronomical units (a.u.)† appears, as well as the corresponding space solar intensity (L). The relationship between R and L is

$$L = (139.6/R^2)\text{mw/cm}^2 \qquad (1)$$

where 139.6 mw/cm² is the accepted value of solar intensity for $R = 1$ (Ref. 4). To compare data from different flights, the values of short-circuit current must be normalized to equal temperature and equal solar intensity. To normalize, the currents are scaled linearly to 140 mw/cm² (rounding off

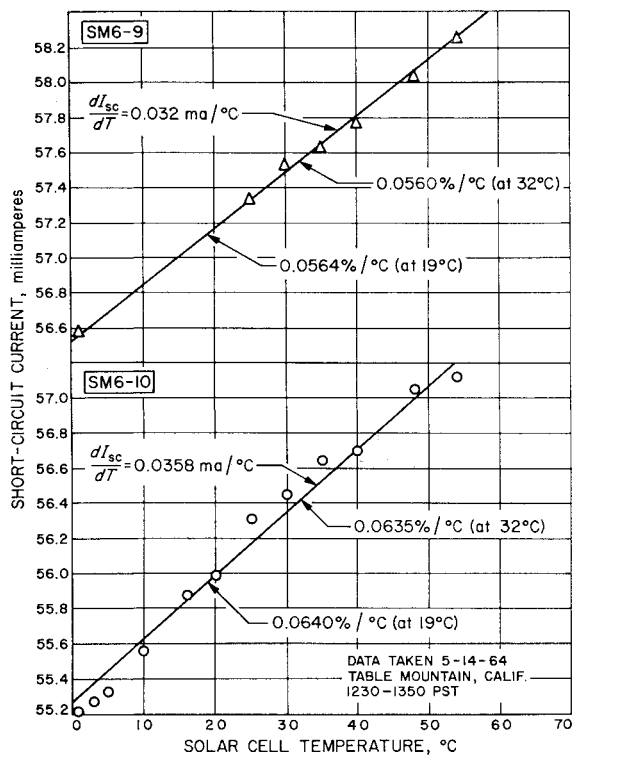

Fig. 11 Short-circuit current vs temperature, SM 6-9 and SM 6-10.

† 1 a.u. = mean distance between the earth and the sun = 149.6 × 10⁶ km.

Table 2 Normalized data and measurement errors for SM 6-9 and SM 6-10

Solar cell	Flight date	Intensity correction[a]	Temperature correction[b]	Normalized values of I_{sc}, ma	Random error (rms deviation), %	Systematic error, %	Total error, %
SM 6-9	6-13-62	1.035	1.005	64.6	±0.28	±0.20	±0.48
	8-6-63	1.032	0.998	64.7	±0.40	±0.20	±0.60
	9-5-63	1.020	0.998	64.1	±0.13	±0.20	±0.33
SM 6-10	6-13-62	1.035	1.006	61.6	±0.29	±0.20	±0.49
	8-6-63	1.032	0.998	61.4	±0.37	±0.20	±0.57
	9-5-63	1.020	0.998	61.2	±0.08	±0.20	±0.28

[a] For 140 mw/cm².
[b] For 28°C.

139.6 mw/cm² to three significant figures) solar intensity and 28°C cell temperature. The temperature dependence of short-circuit current for a constant solar intensity is shown in Fig. 11 for SM 6-9 and SM 6-10. The data in Fig. 11 were obtained in sunlight at Table Mountain, Calif., at an equivalent space solar intensity of about 125 mw/cm². The measurements were made around solar noon, when the solar spectrum is as stable and as close to space sunlight as possible. Table 2 contains the normalizing factors and the normalized values of short-circuit current.

In evaluating the accuracy of the short-circuit current values in Table 2, several sources of error must be considered. The errors may be divided into two groups: 1) random errors, and 2) systematic errors.

The random errors are those that vary over a given series of measurements. These errors are noticeable from the fluctuation in the data points. For a statistically significant set of data, the random error (one-sigma error) may be taken as the rms deviation of the individual values from the mean. The following are possible sources of random errors:

1) Sun-tracker misorientation ($\Delta\theta$) was observed to be less than 3° because of the absence of the off-sun tone during the sampling periods. The maximum error from this source, using a cosine law correction is

$$(\Delta I_{sc}/I_{sc}) \leq 1 - \cos(\Delta\theta) \qquad (2)$$

which gives a maximum of 0.137% deviation for $\Delta\theta = 3°$.

2) The readout error in the telemetry counter-printer/clock system is ±0.093 ma. Using 63.0 ma as a typical value for short-circuit current, the error from this source is

$$\Delta I_{sc}/I_{sc} = \pm 0.093/63.0 = \pm 0.00148 = \pm 0.148\% \qquad (3)$$

3) The measured temperatures are taken as being known to ±1°C. Using the data in Fig. 11, this amounts to an error of less than ±0.1%. Thus, the total random errors are a maximum of +0.385 and −0.248%.

The rms deviations of the measurements listed in Table 1 for the first and second flights exceed the total random error listed previously. This is because of the reflections seen by the solar cells during these flights. For the third flight, the rms deviations in Table 1, as well as the complete set of data as shown in Figs. 9 and 10, are within the given random error limits. The reflections seen on the first two flights were eliminated on the third flight.

The systematic errors are those that remain constant over a series of measurements, thereby acting as a bias in the system. These errors are not evident from the data and can only be evaluated from the sources. They are as follows: 1) the inflight calibration voltages provide a systematic error equal to their calibration accuracy, which is ±0.1%; and 2) the 1-Ω resistor used to load the solar cells is selected to within ±0.1%; the systematic error from this source is, therefore, ±0.1%. The total systematic error is then ±0.2%.

Since the random error for each set of data points is actually observed as the rms deviation, the total error (random plus systematic) may be calculated for each set of data. The total error for each set of data is given in Table 2. The normalized values of space short-circuit current in Table 2 show that the data from the three individual flights were repeated within the accuracy of the measurements.

Conclusions

The data presented in this paper illustrate the feasibility of obtaining space short-circuit current calibrations on solar cells by using high-altitude balloon flights. The accuracy of such calibrations has been shown to be ±0.6%, or better. The calibrations have been shown to be repeatable to within better than ±0.5% for three individual flights flown over a period of more than one year.

References

[1] Zoutendyk, J. A., "A method for predicting the efficiency of solar cell power systems outside the earth's atmosphere," Jet Propulsion Lab., California Institute of Technology, Pasadena, Calif., TR 32-259 (April 1962).

[2] Freier, P. S., Ney, E. P., and Winckler, J. R., "Balloon observation of solar cosmic rays on March 26, 1958," J. Geophys. Res. **64**, 685–688 (1959).

[3] Zoutendyk, J. A., "Solar-cell power systems testing," Jet Propulsion Lab., California Institute of Technology, Pasadena, Calif., TR 32-350 (December 1962).

[4] Johnson, F. S., "The solar constant," J. Meteorol. **11**, 431–439 (1954).